Available online at www.sciencedirect.com
ScienceDirect
Applied Acoustics 70 (2009) 31–40
applied acoustics
www.elsevier.com/locate/apacoust

Estimating the sound absorption coefficients of perforated wooden panels by using artificial neural networks

Min-Der Lin [a], Kang-Ting Tsai [b,*], Bo-Sheng Su [a]

[a] Department of Environmental Engineering, National Chung Hsing University, No. 250 Kuo-Kuang Road, Taichung 402, Taiwan, ROC
[b] Graduate Institute of Rural Planning, National Chung Hsing University, No. 250 Kuo-Kuang Road, Taichung 402, Taiwan, ROC

Received 12 June 2007; received in revised form 24 January 2008; accepted 18 February 2008
Available online 28 March 2008

Abstract

Developing efficient sound absorption materials is a relevant topic for large scale structures such as gymnasiums, shopping malls, airports and stations. This study employs artificial neural network (ANN) algorithm to estimate the sound absorption coefficients of different perforated wooden panels with various setting combinations including perforation percentage, backing material and thickness. The training data sets are built by carrying out a series of experimental measurements in the reverberation room to evaluate the sound absorption characteristics of perforated wooden panels. A multiple linear regression (MLR) model is also developed for making comparisons with ANN. The analytical results indicate that the ANN exhibits satisfactory reliability of a correlation between estimation and truly measured absorption coefficients of approximately 0.85. However, MLR cannot be applied to nonlinear cases. ANN is a useful and reliable tool for estimating sound absorption coefficients estimation.

Keywords: Perforated wooden panel; Sound absorption coefficients; Artificial neural network; Multiple linear regression

1. Introduction

Sound absorber construction comprising a perforated panel with absorptive material and air space backing is widespread as a means of addressing architectural acoustics and noise control problems. There have been numerous studies since that of Bolt in 1947 [1], and the theoretical literature has been built up over approximately 50 years [1–10], for example, Ingard and Bolt [2] reported the acoustic impedance and sound absorption coefficients of perforated panel backing thin porous material and air space; Callaway and Ramer [4] demonstrated the importance of increasing backing material density via experimental measurements; Ingard [5] identified additional acoustic resistance caused by hole flow distortion; Davern [6] discussed the relationship between six factors and the sound absorption coefficient by experimental methods and Zhong and Liu [10] examined the sound absorption characteristics of perforated aluminum panel backing with absorptive material in 1997.

Based on the above literature, investigation and estimation of the sound absorption coefficients of perforated panels in an important topic in the research on acoustics. However, based on the literature to date, currently the only means of obtaining the sound absorption characteristics of a certain perforated panel configuration is via realistic experimental measurements. Consequently it is very cumbersome to examine the optimal configuration of the sound absorber construction that offers the best sound absorption characteristics, especially when the configuration contains numerous compositions. This situation suggests that accurate sound absorption estimation models are necessary.

Artificial neural networks have attracted growing attentions in academia and been employed in many studies involving empirical data analysis. This study thus performs a series of experimental measurements in a reverberation room to assess the sound absorption characteristics of

* Corresponding author. Tel.: +886 4 22850403; fax: +886 4 22859645.
E-mail address: kttsai@nchu.edu.tw (K.-T. Tsai).

0003-682X/$ - see front matter © 2008 Elsevier Ltd. All rights reserved.
doi:10.1016/j.apacoust.2008.02.001

perforated wooden panels, and then employs ANN to develop a model capable of accurately estimating the absorption coefficients of perforated wooden panels in different settings.

2. Artificial neural network

Artificial neural network (ANN) is a mathematical model whose architecture and functional form is based on a simulation of the human brain system. ANN is widely used in nonlinear models that have been widely applied to pattern recognition and system identification [11]. One feature of the ANN model is its ability to adapt to recurrent changes and detect patterns in complex natural systems. Another feature is its self-learning capability [12,13].

ANN is an interconnected parallel structure containing neurons, which are simple processing elements. The neurons contained in ANN are usually arranged in a series of layers. A typical ANN model generally comprises an input layer, an output layer, separated by at least one hidden layer. Fig. 1 illustrates a typical three-layered ANN with '*I*' input neurons, '*H*' hidden neurons and '*O*' output neurons. The circles represent nodes (neuron) and the arrows represent the unidirectional interconnections between them. Hidden layers serve as feature detectors, and universal approximation theory [14] maintains that a single-hidden-layer ANN with sufficient neurons can map any input to any output, with an arbitrary degree of accuracy [15]. Wang et al. [16] concluded that the number of input and output neurons is determined by the data complexity of the problem being investigated, in addition to which the hidden neuron number is also problem-specific. Although several empirical rules have been proposed, optimizing the number of layers and neurons is still done through trial and error.

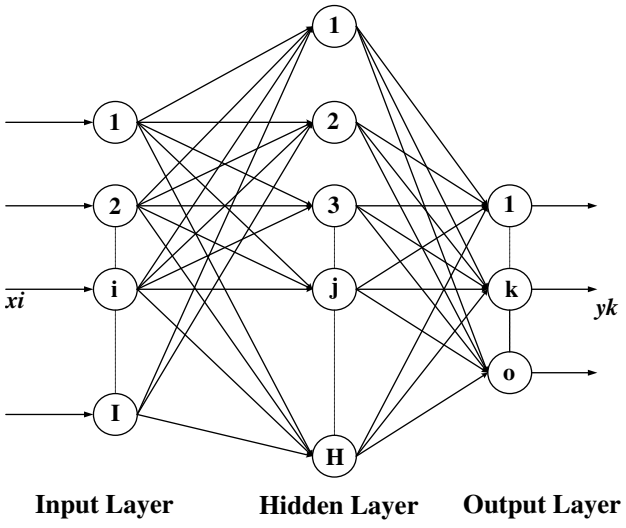

Fig. 1. Illustration of a typical artificial neural network.

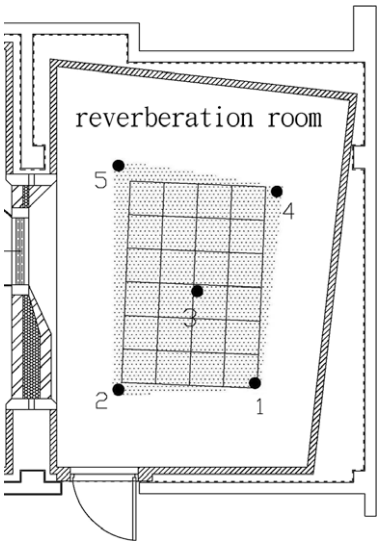

Fig. 3. Sound absorption coefficient measurement setting.

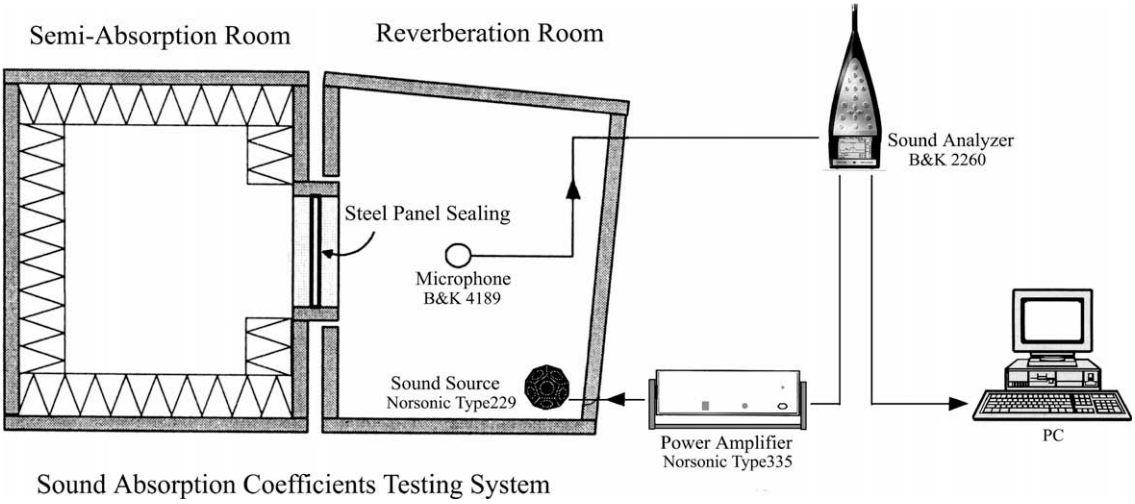

Fig. 2. Measurement system in the reverberation room.

The neurons in the input layer represent the input variables (such as, independent variables) that receive inputs from the external environment. The output layer contains a single neuron for each output (for example, dependent variable). The hidden layer possesses features of learning rule and activity transfer function. The neurons in the first hidden layer (layer 2) receive input variables from the input layer (layer 1) and manipulate them in the form of a weighted summation, as defined in Eq. (1). Meanwhile, the second hidden and output neurons receive outputs from all of the neurons in the preceding layer, and a weighted summation is also calculated as defined in Eq. (2). The information is then passed through a 'S'-shaped logistic sigmoid transfer function, as defined in Eq. (3) to generate an output [17].

$$S_i^2 = \sum_{k=1}^{n} w_{ki} \cdot x_k - \theta_i \tag{1}$$

$$S_i^j = \sum_{k=1}^{N^{j-1}} w_{ki} \cdot y_k^{j-1} - \theta_i \quad j \geqslant 3 \tag{2}$$

$$y_i^j = \frac{1}{1 + e^{-S_i^j}} \quad j \geqslant 2 \tag{3}$$

where S_i^j denotes the weighted summation of the ith neuron in the jth layer; n represents the number of input variables; x_k is the kth input variable; N^{j-1} denotes the number of neurons in the $(j-1)$th layer; w_{ki} represents the linking-weighted value between neuron i and k; y_i^j is the output value of the ith neuron in the jth layer; and θ_i is the threshold value. Furthermore, the input–out data must be normalized to ensure it remains within the same range as the transfer function used. The input data are normalized using their minimum and maximum values to avoid overflow resulting from extremely large or extremely small weights. The output is eventually transformed back to the original full range of values for purpose of interpreting the results.

An ANN model comprises training and testing stages. The training procedure of ANN is an optimization process in which an error function is minimized by adjusting the weight w_{ki}. This study employs the most popular back-propagation algorithm in training. During training, a set of n pairs of input vectors ($\boldsymbol{X}_i$) and corresponding target outputs ($\boldsymbol{T}_i$), $\{(\boldsymbol{X}_1, \boldsymbol{T}_1), (\boldsymbol{X}_2, \boldsymbol{T}_2), \ldots, (\boldsymbol{X}_n, \boldsymbol{T}_n)\}$, is presented to the network one pair at a time and an corresponding predicted output is calculated. This predicted output is

Table 1
Summary of network architectures of the ANN models

Case	Network architecture (input–hidden–output)	Testing set		
		r	r^2	RMSE (NRC)
DF1	3–8–1	0.7700	0.5929	0.0562
DF2	3–15–1	0.8325	0.6930	0.1656
DF3	3–8–8–1	0.8342	0.6959	0.1349
SPF1	3–8–8–1	0.8404	0.7063	0.0391
SPF2	3–8–8–1	0.8480	0.7191	0.1375
SPF3	3–3–1	0.8376	0.7016	0.1392
WRC1	3–10–10–1	0.8146	0.6636	0.0020
WRC2	3–8–8–1	0.8618	0.7427	0.1328
WRC3	3–3–1	0.8630	0.7448	0.1378

Table 2
Summary of multiple linear regression models for different perforated wooden panels

Case	Multiple Linear Regression Models	r^2
DF1	$4.65 \times 10^{-2} + 3.675 \times 10^{-2} \cdot X_1 + 1.421 \times 10^{-3} \cdot X_2 + 2.012 \times 10^{-5} \cdot X_3$	0.0212
DF2	$0.722 - 3.068 \times 10^{-2} \cdot X_1 + 1.873 \times 10^{-2} \cdot X_2 - 1.370 \times 10^{-4} \cdot X_3$	0.6083
DF3	$0.739 - 2.834 \times 10^{-2} \cdot X_1 + 1.577 \times 10^{-2} \cdot X_2 - 1.292 \times 10^{-4} \cdot X_3$	0.5707
SPF1	$8.581 \times 10^{-2} + 7.154 \times 10^{-3} \cdot X_1 - 5.282 \times 10^{-4} \cdot X_2 + 1.384 \times 10^{-5} \cdot X_3$	0.0009
SPF2	$0.742 - 3.450 \times 10^{-2} \cdot X_1 + 1.696 \times 10^{-2} \cdot X_2 - 1.431 \times 10^{-4} \cdot X_3$	0.5747
SPF3	$0.768 - 3.145 \times 10^{-2} \cdot X_1 + 1.314 \times 10^{-2} \cdot X_2 - 1.354 \times 10^{-4} \cdot X_3$	0.5783
WRC1	$5.124 \times 10^{-2} + 2.875 \times 10^{-2} \cdot X_1 + 2.654 \times 10^{-4} \cdot X_2 + 1.544 \times 10^{-5} \cdot X_3$	0.023
WRC2	$0.732 - 3.096 \times 10^{-2} \cdot X_1 + 1.765 \times 10^{-2} \cdot X_2 - 1.324 \times 10^{-4} \cdot X_3$	0.5902
WRC3	$0.759 - 2.674 \times 10^{-2} \cdot X_1 + 1.392 \times 10^{-2} \cdot X_2 - 1.250 \times 10^{-4} \cdot X_3$	0.5669

Table 3
Statistics of absorption coefficients estimation via the ANN and MLR

Statistic	Unit	DF1	DF2	DF3	SPF1	SPF2	SPF3	WRC1	WRC2	WRC3
Measured (means)	NRC	0.139	0.547	0.562	0.110	0.523	0.540	0.111	0.543	0.548
MAE (ANN)	NRC	0.045	0.145	0.111	0.032	0.105	0.114	0.036	0.104	0.118
MAE (MLR)	NRC	0.085	0.145	0.123	0.069	0.130	0.122	0.071	0.115	0.105
RMSE (ANN)	NRC	0.056	0.165	0.134	0.039	0.137	0.139	0.001	0.132	0.137
RMSE (MLR)	NRC	0.098	0.155	0.153	0.082	0.153	0.154	0.007	0.143	0.137
r (ANN)		0.77	0.83	0.83	0.84	0.84	0.83	0.81	0.86	0.86
r (MLR)		**0.05**	0.79	0.76	**0.03**	0.79	0.80	**0.03**	0.80	0.77
r^2 (ANN)		0.592	0.693	0.695	0.706	0.719	0.701	0.663	0.742	0.744
r^2 (MLR)		**0.002**	0.633	0.587	**0.001**	0.634	0.642	**0.001**	0.644	0.607

then compared with the target output, and an error function expressed as the mean squared error E is defined as

$$E = \frac{1}{2}\sum_{k}(T_k - y_k)^2 \tag{4}$$

where T_k denotes the target output value of the dependent variable k, and y_k represents the corresponding predicted output of ANN. The error function is then used to adjust the weights w_{ki} by back-propagating the errors from the output layer back into the whole network. The adjusting procedure is repeated iteratively until the allowable or minimal error is achieved. Simultaneously, a "learning rate" or "learning coefficient", η, is also required to regulate the convergence speed of error minimization. Adequate η is necessary to avoid rapid learning or over-fitting [18]. Haykin [19] explains and presents the mathematics of back-propagation algorithm in more detail.

3. Experiments for sound absorption data measurement

A set of realistic measurement data of the sound absorption coefficients is necessary for developing the ANN model. The sound absorption data measurements used in this study follow the CNS (Chinese National Standards) 9065 "Method for Measurement of Sound Absorption Coefficients in a Reverberation Room". All of the measurements were conducted in the reverberation room of the acoustic laboratory located in the Department of Architecture, National Cheng Kung University, Tainan, Taiwan. The reverberation room had floor area of 32.8 m^2, empty volume of 171.6 m^3, and interior surface area of 184.3 m^2. Sound pressures were measured to determine the sound attenuation in the room. The dimensions of the room indicated a cutoff frequency of 125 Hz. A real time analyzer (B&K 2260) was used to measure the sound

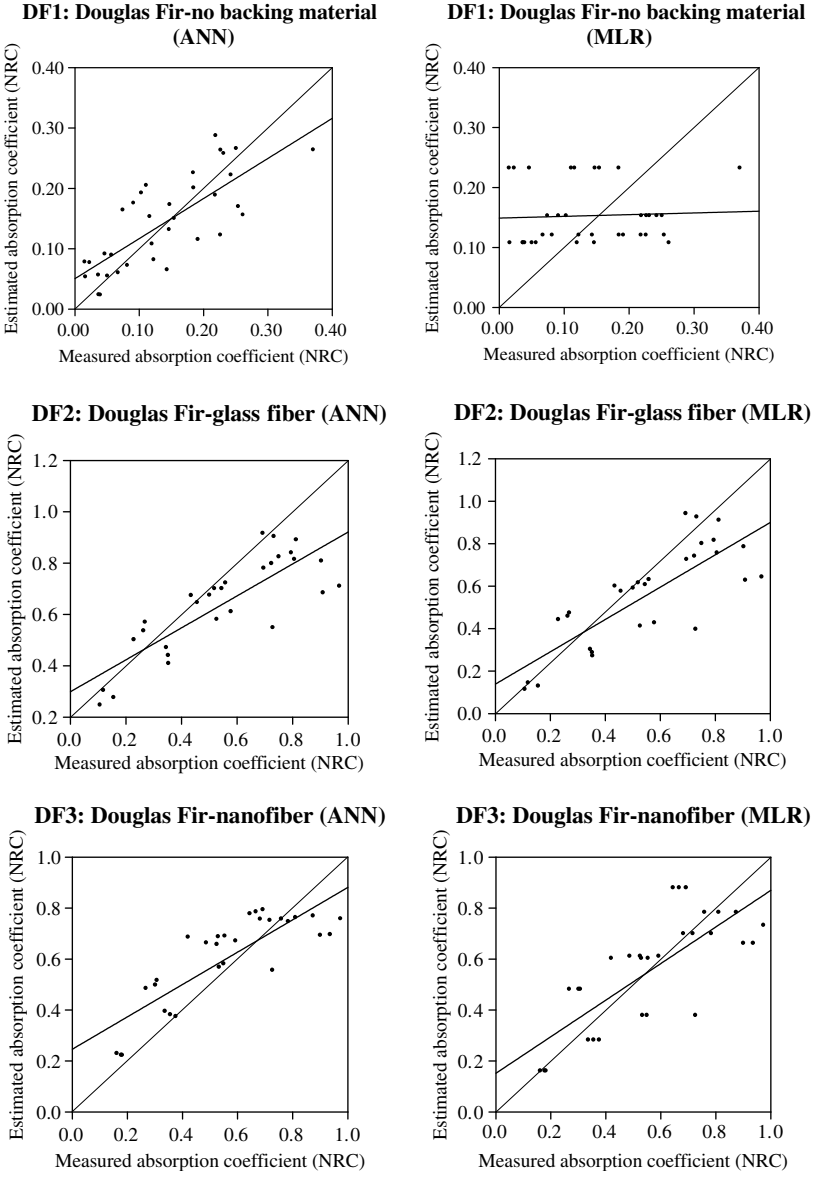

Fig. 4. Cross plots of estimated and measured absorption coefficients of DF.

attenuation in the reverberation room, meaning the reverberation time. One port of the analyzer was connected to the sound source (Nor sonic Type 229) to control the speaker sound while the other port was connected to the microphone (B&K 4189) to receive the sound attenuation signals. Fig. 2 shows the layout of the measurement system in the reverberation room.

The testing specimen of the perforated wooden panel used in this work had length 4.2 m, width 2.856 m and area 12 m^2. The length/width ratio was thus 1.47, conforming to CNS A3165. The distance from each side of the specimen to the reverberation room walls exceeded 1 m. Each measurement was performed with microphones placed at five fixed points, as illustrated in Fig. 3. Individual sound absorption coefficients were then obtained by averaging the measurements at the five fixed points. The number of tests and records was consistent with CNS A3165.

The reverberation times for each frequency were measured in both the empty and test specimen filled reverberation room. The sound absorption coefficient was then calculated using Eq. (5)

$$\alpha = \frac{55.3V}{C \cdot S}\left(\frac{1}{T_1} - \frac{1}{T_2}\right) \tag{5}$$

where α denotes the sound absorption coefficient; V represents the volume of the empty reverberation room (m^3); C is the velocity of sound in air (m/s); S denotes the area of the test specimen (m^2); T_1 is the reverberation time following the introduction of the test specimen (s); and T_2 is the reverberation time for the empty reverberation room (s). Three wooden perforated panels made of douglas fir (DF), spruce fir pine (SFP) and western red cedar (WRC) with different backing situations, namely "no backing material", "glass fiber backing" and "nanofiber backing",

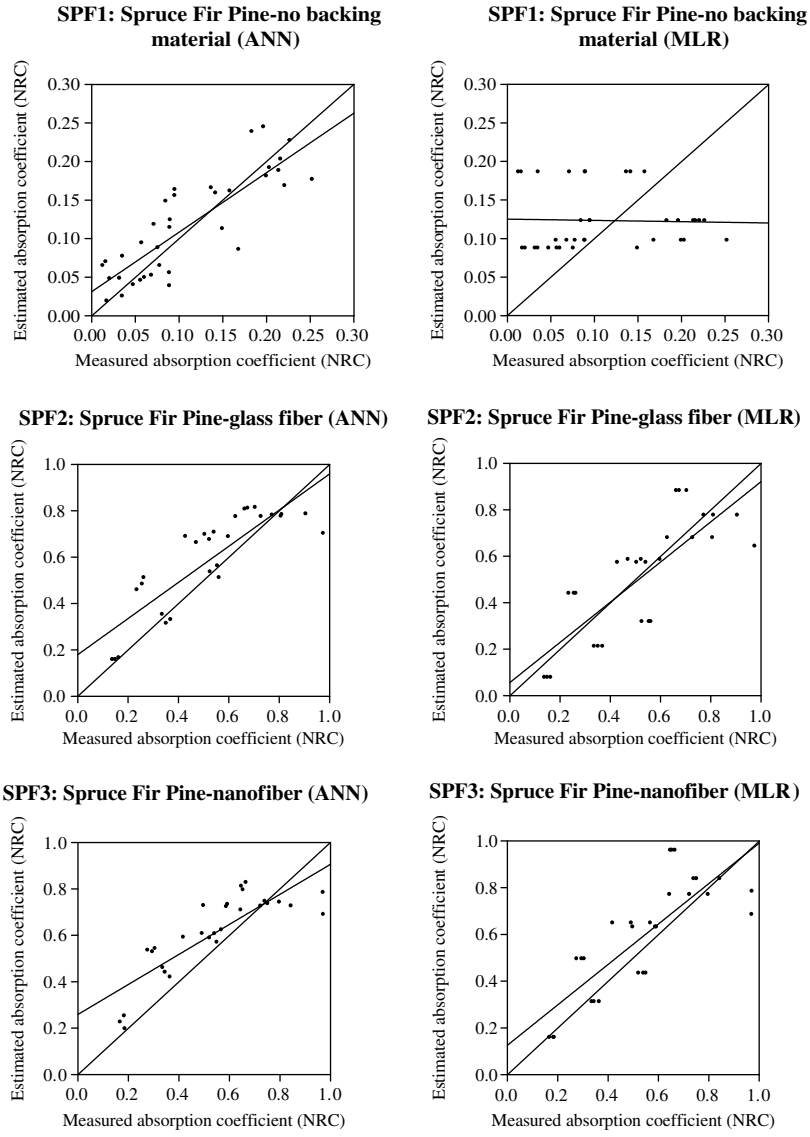

Fig. 5. Cross plots of estimated and measured absorption coefficients of SPF.

were investigated to determine the absorption coefficients of different frequencies with various panel thickness and panel perforation percentage. More than 1200 records were collected during the series of experiments.

4. Model development

4.1. Artificial neural network building

The sound absorption coefficient data of DF, SPF and WRC for three different settings (that is, no backing material, glass fiber backing and nanofiber backing) obtained from the above reverberation room were used individually to develop their own ANN models. This approach resulted in nine data sets. Each data set was randomly divided into two groups: 75% of the data (total number of 108 records) were used for network training with the remainder (a total of 36 records) for network testing. Since absorption coefficient variation can be a function of frequency, panel perforation percentage and panel thickness, three neurons of the ANN input layer are used to represent these three independent variables. The output layer contains just one neuron, corresponding to the only dependent variable, the sound absorption coefficient. The ANN program developed by Neuralware, Inc., *Neural Works Professional II/PLUS®* was employed in this study to build the ANN models.

Hundreds of trials were conducted to optimize the configurations of the number of hidden layers, number of neurons in each hidden layer and learning rate so as to achieve accurate predictions. Table 1 lists the nine network

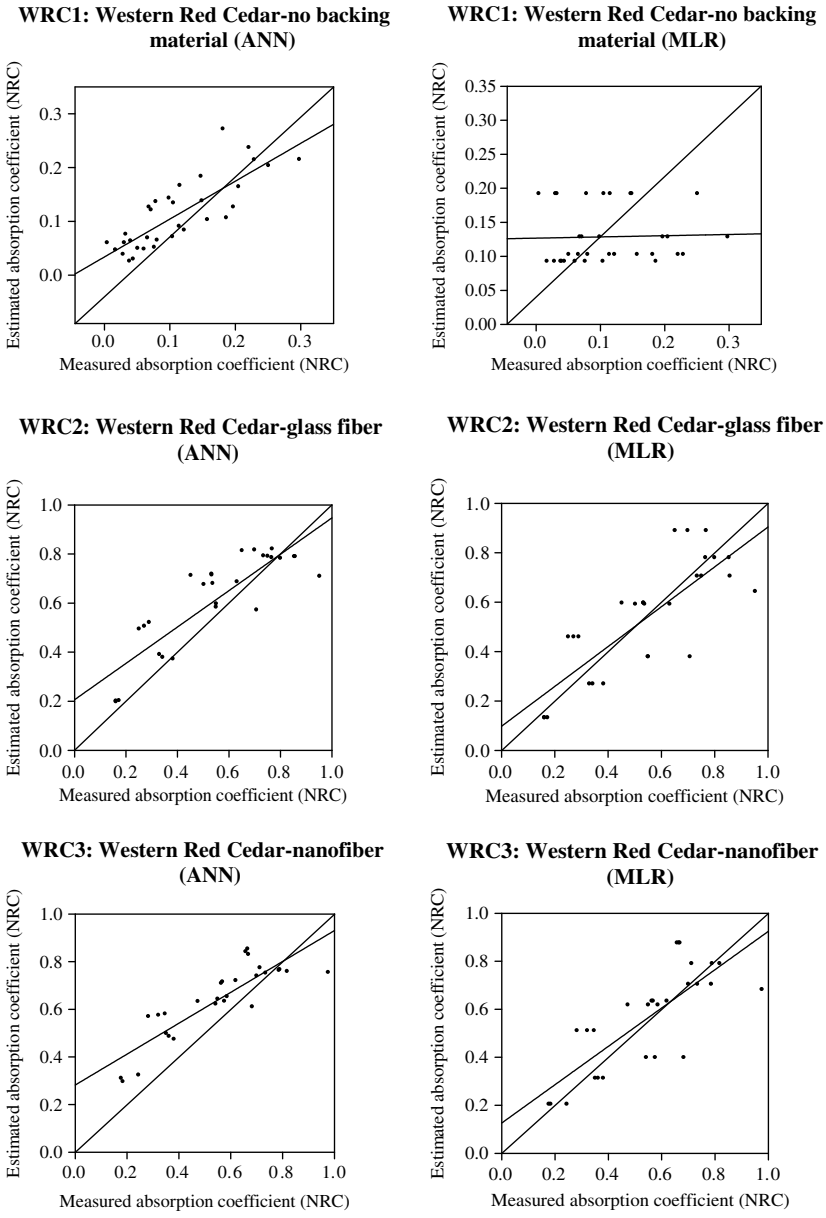

Fig. 6. Cross plots of estimated and measured absorption coefficients of WRC.

architectures that optimized the prediction results. The Case indexes 1, 2 and 3 represent the settings "no backing material", "glass fiber backing" and "nanofiber backing", respectively. Regarding the network architecture notation, 3–8–1 denotes three neurons in the input layer, eight in the hidden layer and one in the output layer. A double hidden layer would be indicated by the notation 3–8–8–1.

4.2. Multiple linear regression model building

The sound absorption coefficients estimated via ANN were also compared with those estimated using the multiple linear regression (MLR) model to further assess their accuracy. The MLR model for absorption coefficients was formulated as a function of the same three independent variables (perforation percentage, thickness and frequency) used in the ANN, enabling a direct comparison with the results obtained using the ANN models. Least-squares analysis was carried out to obtain the linear equation that best fitted the measured absorption coefficients. The equations listed in Table 2 were found to yield the best-fit of each case. The coefficients of correlation (r^2) were also listed.

To assess the estimation performance of the ANN and MLR models, this study used the root mean square error (RMSE) and coefficients of determination (r^2), as described in the following equations. The mean absolute error (MAE), calculated as the average absolute value of the deviation between the estimated and measured values, was also employed.

$$\mathrm{RMSE} = \sqrt{\frac{\sum_{j=1}^{N}(T_j - Y_j)^2}{N}} \tag{6}$$

$$r^2 = 1 - \frac{\sum (T_j - Y_j)^2}{\sum T_j^2 - \frac{\sum Y_j^2}{N}} \tag{7}$$

where T_j and Y_j denotes the measured and estimated values of data i, respectively; and N represents the number of measurements. Furthermore, RMSE and MAE indicate the estimation accuracy. Estimations with lower RMSE and MAE values represent more accurate results. Meanwhile, r^2 indicates the similarity between the model tendency and the measured data, with higher r^2 value representing greater similarities.

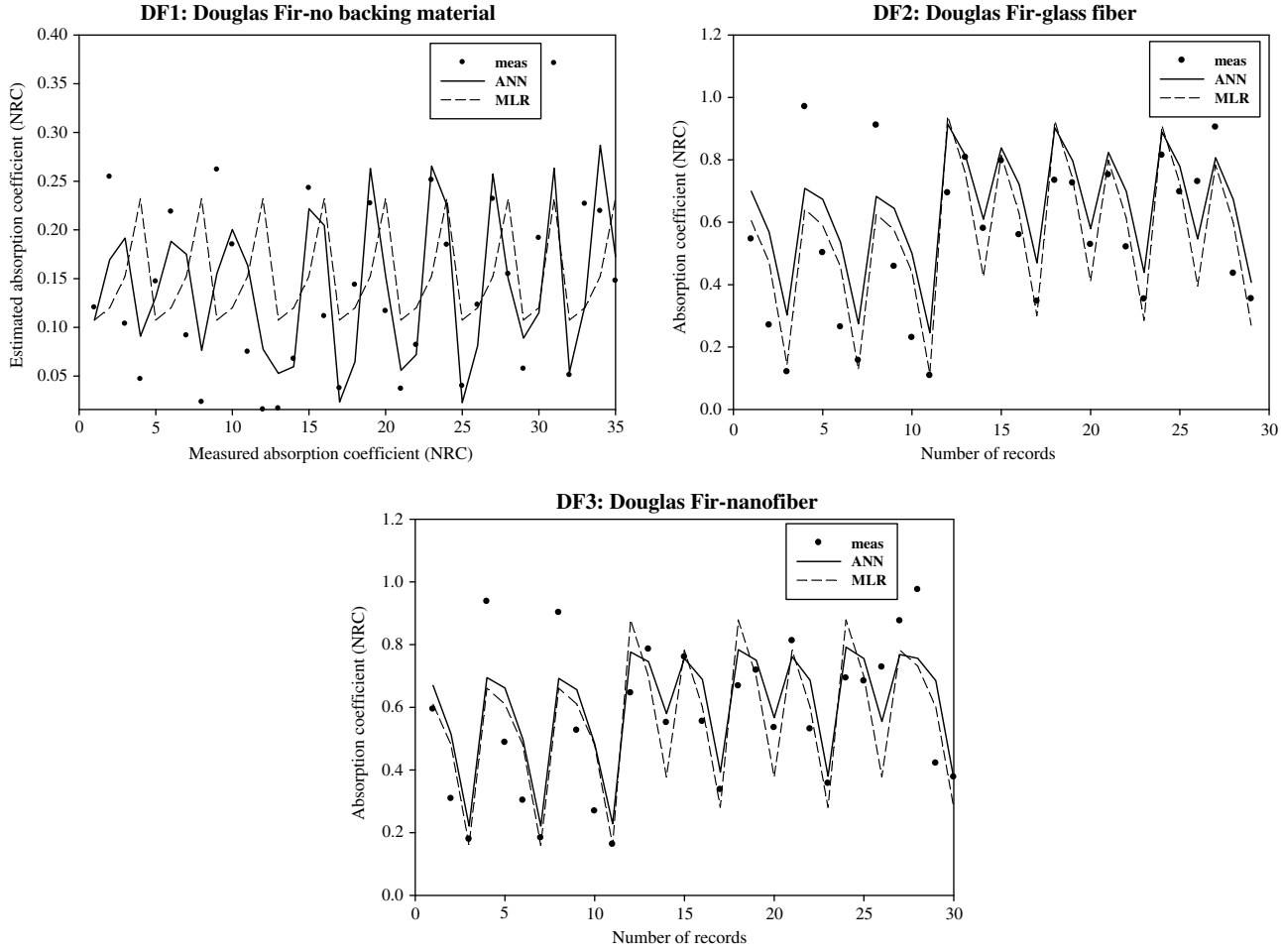

Fig. 7. Comparison of absorption coefficient estimation models (for douglas fir).

5. Results and discussion

Following the development of the ANN and MLR models, the testing set data were used to examine the effectiveness of the models in estimating absorption coefficients. The estimation performance of each model was evaluated and compared for each case using statistical and graphical comparisons. The measured sound absorption coefficients for the nine cases ranged from 0.005 NRC in WRC1 to 0.977 NRC in WRC3, while the means ranged from 0.110 NRC in SPF1 to 0.562 NRC in DF3, as listed in Table 3. The comparative statistics summarized in Table 3 reveal that for most of the cases the ANN models achieve higher correlation coefficients (r) and smaller MAE and RMSE, and therefore outperform MLR. However, the performances of ANN and MLR did not differ substantially except for cases DF1, SPF1 and WRC1.

Figs. 4–6 illustrate cross plots of estimated (including ANN and MLR) and measured sound absorption coefficients for the testing set data. The two diagonal lines on the plots represent the best-fit regression line through the data and the line of perfect correspondence between the measurements and estimations. The illustrations demonstrate that although both the ANN and MLR models overestimate the low values and underestimate the high values of absorption coefficients, both methods can yield satisfactory estimations except in the situations where MLR is used to estimate "no backing material" cases. For all of the cases where no backing material is involved, namely, cases DF1, SPF1 and WRC1, the MLR models perform very poorly. These finding agree with the conclusion of Ingard and Bolt [2] that the sound absorption behavior of perforated wooden panels with no backing material exhibits nonlinear characteristics that prevent it being formulated via linear regressions. ANN models outperform MLR because ANN is suitable for both linear and nonlinear problems.

To further assess the accuracy of the ANN and MLR models, Figs. 7–9 plot the estimated and measured sound absorption coefficients versus the testing records. Clearly, some extreme values could not be accurately estimated by either the ANN or MLR models. This phenomenon occurs because records of extreme values are rare in the training data set, resulting in the relatively poor ability for the two methods to capture extreme values.

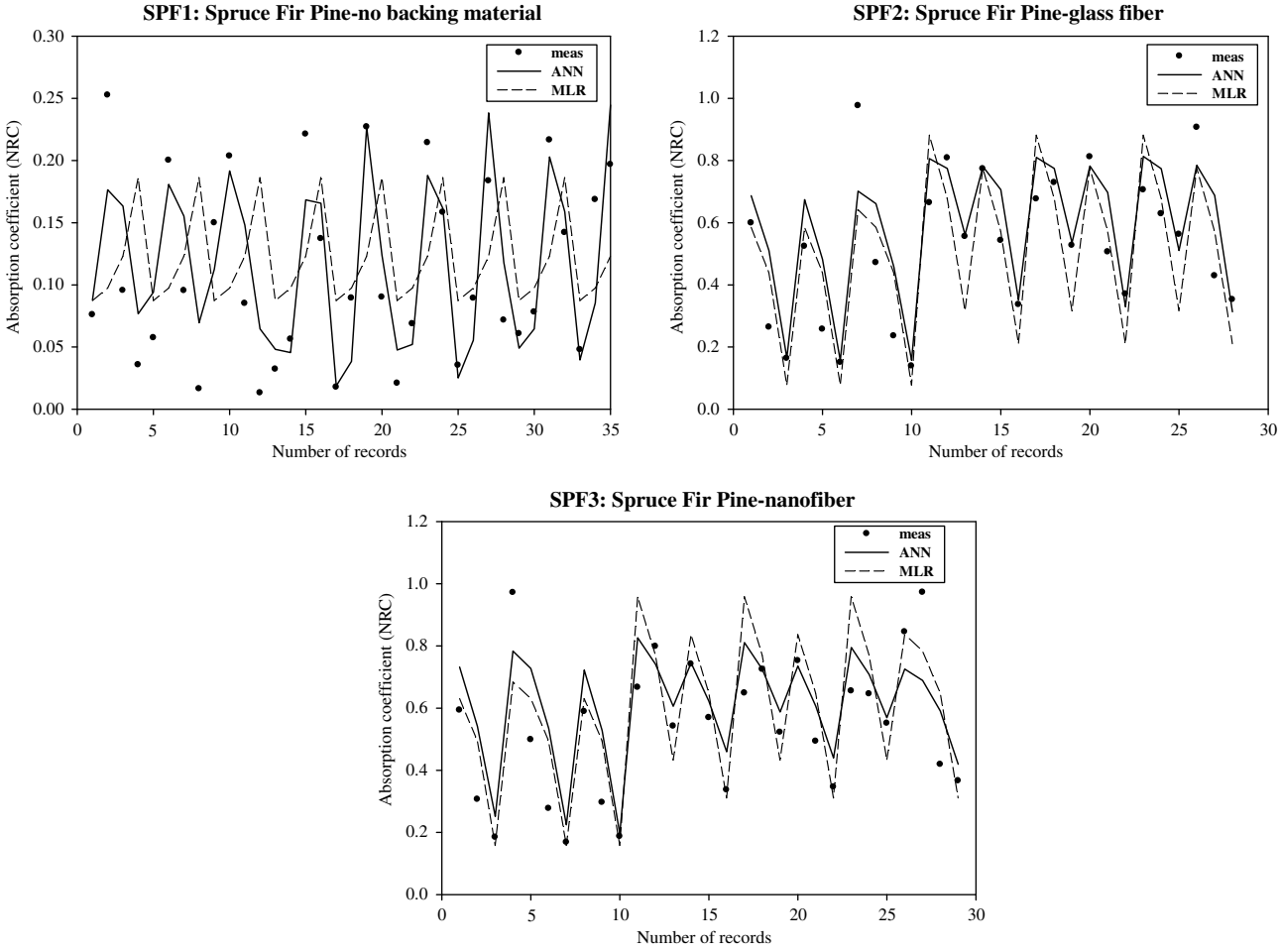

Fig. 8. Comparison of absorption coefficient estimation models (for spruce fir pine).

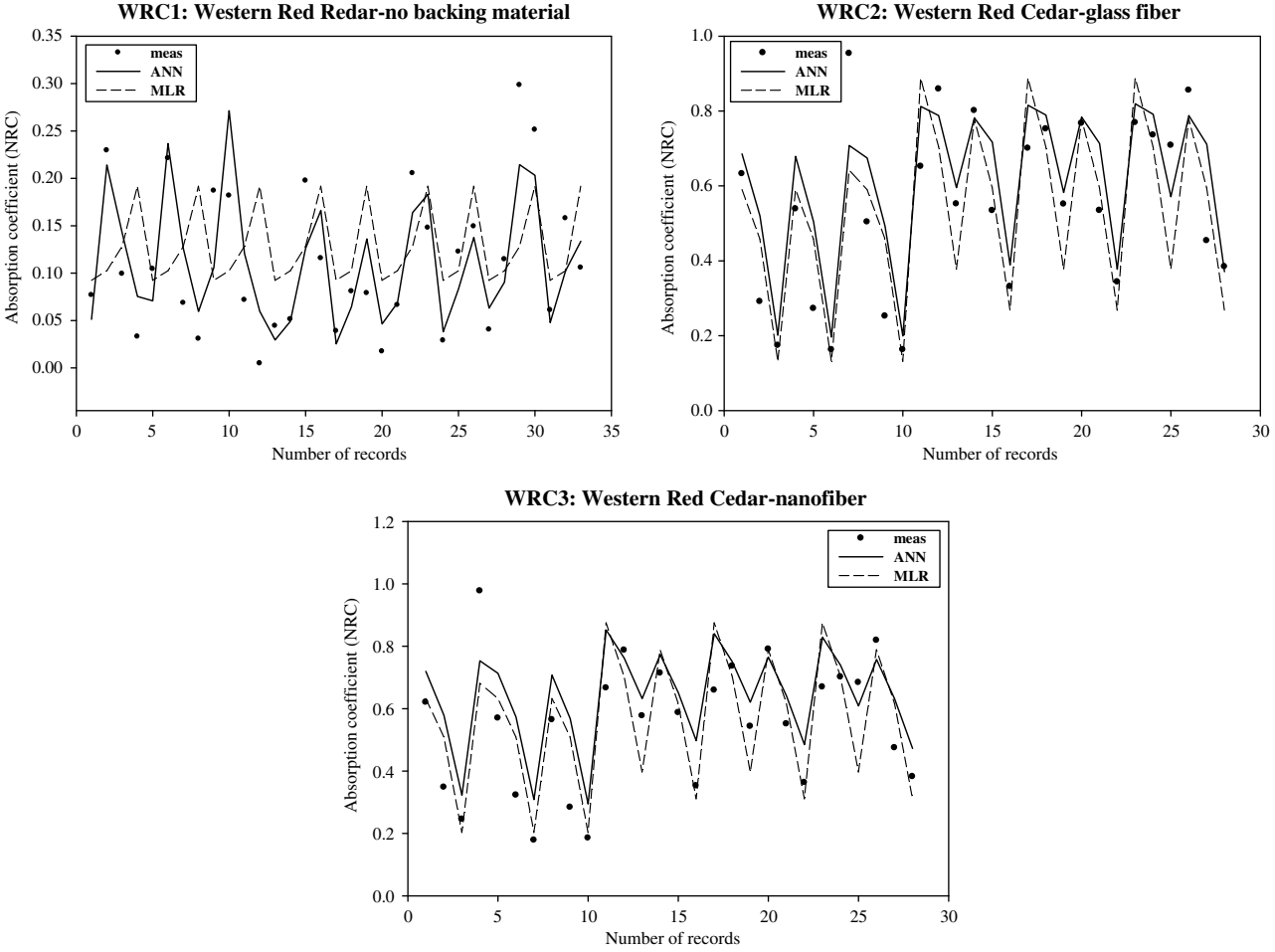

Fig. 9. Comparison of absorption coefficient estimation models (for western red cedar).

6. Conclusions

This study conducts an initial investigation of the potential use of ANN for estimating the sound absorption coefficients of perforated wooden panels. Three wooden materials (douglas fir, spruce fir pine and western red cedar) with three different settings (no backing material, glass fiber backing and nanofiber backing) were served as case studies. The results of a feed-forward ANN employing a back-propagation algorithm were also compared with those of the MLR model. All of the models were based on data from actual measurements of absorption coefficients gathered from a series of experiments carried out in the reverberation room.

Comparison of the two estimation approaches revealed that since the sound absorption behavior of perforated wooden panels with no backing material exhibits higher nonlinear characteristics, the absorption coefficients estimated by ANN are significantly better than those obtained using MLR. However, for other cases the estimation of the absorption coefficients by both ANN and MLR show satisfactory reliability, with the correlations with actual measurements of absorption coefficients being approximately 0.85 and 0.80, respectively. This study thus concludes that ANN slightly outperforms MLR owing to the fact that ANN is able to manage both linear and nonlinear problems.

Besides the assessment of performances, other modeling issues also deserve consideration. First, this study included only three independent variables (perforation percentage, thickness and frequency). While these variables represent a satisfactory starting point, models that consider other/more variable constructs are appropriate areas for future works. Second, this work only used one type of ANN architecture. Further research thus could focus on employing other network types.

Acknowledgements

The authors would like to thank the Council of Agriculture of the Republic of China, Taiwan for financially supporting this research under a Canada-Taiwan collaborative project on agricultural technology (Grant No.: 93-Nong-Ke-1.4.1-CO-I9). Special thanks also go to the anonymous reviewers for their precious opinions which help improve this work.

References

[1] Bolt RH. On the design of perforated facings for acoustic materials. J Acoust Soc Am 1947;19:917–21.

[2] Ingard KU, Bolt RH. Absorption characteristics of acoustic material with perforated facings. J Acoust Soc Am 1951;23:533–40.

[3] Beranek LL. Acoustical measurements. Publisher for the Acoustical Society of American by American Institute; 1949.

[4] Callaway DB, Ramer LG. The use of perforated facings in designing low frequency resonant absorbers. J Acoust Soc Am 1952;24:309–12.

[5] Ingard KU. Perforated facing and sound absorption. J Acoust Soc Am 1954;26:151–4.

[6] Davern WA. Perforated facings backed with porous materials as sound absorbers-an experimental study. Appl Acoust 1977;10:85–112.

[7] Kuttruff H. Room acoustics. third ed. London and New York: Elsevier Applied Science; 1991.

[8] Beranek LL, Vér IL. Noise and vibration control engineering. John Wiley & Sons, Inc.; 1992.

[9] Takahashi D. A new method for predicting the sound absorption of perforated absorber systems. Appl Acoust 1997;51:71–84.

[10] Zhong XZ, Liu JK. Absorption properties of perforate decorative aluminum ceiling strips. Tech Acoust 1997;16:69–75.

[11] Fu C, Poch M. System identification and real-time pattern recognition by neural networks for an activated sludge process. Environ Int 1995;21(1):57–69.

[12] Spall JC, Cristion JA. A neural network controller for treatment. IEEE Trans Syst, Man Cybernet Part B: Cybernet 1997;27(3):369–75.

[13] Lee DS, Park JM. Neural network modeling foe on-line estimation of nutrient dynamics in a sequentially operated batch reactor. J Biotechnol 1999;75:229–39.

[14] Tampe SS, Kulkarni BD, Desphande PB. Elements of artificial networks with selected applications in chemical engineering, and chemical and biological sciences. Louisville (KY, USA): Simulation and Advanced Controls, Ltd.; 1996.

[15] Elkamel A, Abdul-Wahab S, Bouhamra W, Alper E. Measurement and prediction of ozone levels around a heavily industrialized area: a neural network approach. Adv Environ Res 2001;5:47–59.

[16] Wang Z, Massimi CD, Tham MT, Morris AJ. A procedure for determining the topology of multilayer feed-forward neural networks. Neural Networks 1994;7:291–300.

[17] Wieland D, Wotawa F, Wotawa G. From neural networks to qualitative models in environmental engineering. Comput-Aided Civil Infrastruct Eng 2002;17:104–18.

[18] Spellman G. An application of artificial neural networks to the prediction of surface ozone concentrations in the United Kingdom. Appl Geogr 1999;19:123–36.

[19] Haykin S. Neural networks: a comprehensive foundation. New Jersey: Prentice Hall; 1998.